

# Cardiac Computed Tomography Radiomics A Comprehensive Review on Radiomic Techniques

Márton Kolossváry, MD,\* Miklós Kellermayer, MD, PhD, DSc,†  
Béla Merkely, MD, PhD, DSc,\* and Pál Maurovich-Horvat, MD, PhD, MPH\*

**Abstract:** Radiologic images are vast three-dimensional data sets in which each voxel of the underlying volume represents distinct physical measurements of a tissue-dependent characteristic. Advances in technology allow radiologists to image pathologies with unforeseen detail, thereby further increasing the amount of information to be processed. Even though the imaging modalities have advanced greatly, our interpretation of the images has remained essentially unchanged for decades. We have arrived in the era of precision medicine where even slight differences in disease manifestation are seen as potential target points for new intervention strategies. There is a pressing need to improve and expand the interpretation of radiologic images if we wish to keep up with the progress in other diagnostic areas. Radiomics is the process of extracting numerous quantitative features from a given region of interest to create large data sets in which each abnormality is described by hundreds of parameters. From these parameters datamining is used to explore and establish new, meaningful correlations between the variables and the clinical data. Predictive models can be built on the basis of the results, which may broaden our knowledge of diseases and assist clinical decision making. Radiomics is a complex subject that involves the interaction of different disciplines; our objective is to explain commonly used radiomic techniques and review current applications in cardiac computed tomography imaging.

**Key Words:** radiomics, cardiovascular disease, cardiac computed tomography

(*J Thorac Imaging* 2018;33:26–34)

Medical imaging has developed exponentially in the past decades.<sup>1</sup> Although new techniques are frequently introduced for each imaging modality, in daily clinical routine the interpretation of medical images is still based mainly on qualitative image characteristics. State-of-the-art scanners can achieve submillimeter spatial and millisecond temporal resolution, significantly increasing the

amount of information gained from radiologic examinations. Qualitative evaluation of medical images discards vast amounts of information while relying on hard-to-reproduce and greatly subjective expert opinion.<sup>2</sup> For most cases, this kind of image interpretation might be sufficient for clinical judgment, but in the era of precision medicine, when we seek to refine our taxonomy of diseases and cure illnesses on the basis of subtle differences in the clinical and pathologic manifestation of diseases,<sup>3</sup> much more is expected from radiology, the medical profession of imaging pathologies.

Radiologic images are in fact extensive two-dimensional or three-dimensional (2D or 3D) data sets in which the quantitative values present in the pixels (or volumetric pixels called voxels) are used to create a picture. Each and every voxel is a measurement itself on the basis of some physical characteristics of the underlying anatomic structure, such as the attenuation of electromagnetic radiation intensity that is used in computed tomography (CT). These values can be assessed by visual inspection, as done in daily clinical routine, or they can be analyzed using advanced image analyses. Radiomics is the process of extracting numerous quantitative features from a given region of interest to create large data sets in which each abnormality is described by hundreds of parameters. Some of these parameters are commonly known and used by radiologists, such as the mean attenuation value or the longest diameter of a lesion, whereas others that quantify the heterogeneity or shape of an abnormality are less apparent. From these values novel analytical methods are used to identify associations between the parameters and the clinical or outcome data. Datamining is the process of finding new, meaningful patterns and relationships between the different variables. From these results, novel imaging biomarkers may be identified that can increase the diagnostic accuracy of radiologic examinations and expand our knowledge of the underlying pathologic processes (Fig. 1).

Our objective is to summarize commonly used image analytical methods in radiomics and review current applications of these techniques in cardiovascular radiology.

## IDEA BEHIND CORONARY CT RADIOMICS

Coronary lesions are complex pathologies made up of several different histologic components. Each of the different tissues involved absorbs radiation to a different extent; thus they are depicted as having different attenuation values on CT. Basically, each voxel is a separate measurement of how much radiation is absorbed in the given volume; thus, CT can be used to evaluate the underlying anatomic structure in vivo. Therefore, it is rational to assume that distinct morphologies of different coronary lesions appear differently in CT. As a result,

From the \*MTA-SE Cardiovascular Imaging Research Group, Heart and Vascular Center; and †Department of Biophysics and Radiation Biology, Semmelweis University, Budapest, Hungary.

Supported by the National Research, Development and Innovation Office of Hungary (NKFI; NVKP-16-1-2016-0017).

The authors declare no conflicts of interest.

Correspondence to: Pál Maurovich-Horvat, MD, PhD, MPH, MTA-SE Cardiovascular Imaging Research Group, Heart and Vascular Center, Semmelweis University, 68, Városmajor Street, 1122 Budapest, Hungary (e-mail: p.maurovich.horvat@mail.harvard.edu).

Copyright © 2017 The Author(s). Published by Wolters Kluwer Health, Inc. This is an open-access article distributed under the terms of the Creative Commons Attribution-Non Commercial-No Derivatives License 4.0 (CCBY-NC-ND), where it is permissible to download and share the work provided it is properly cited. The work cannot be changed in any way or used commercially without permission from the journal.

DOI: 10.1097/RTI.0000000000000268

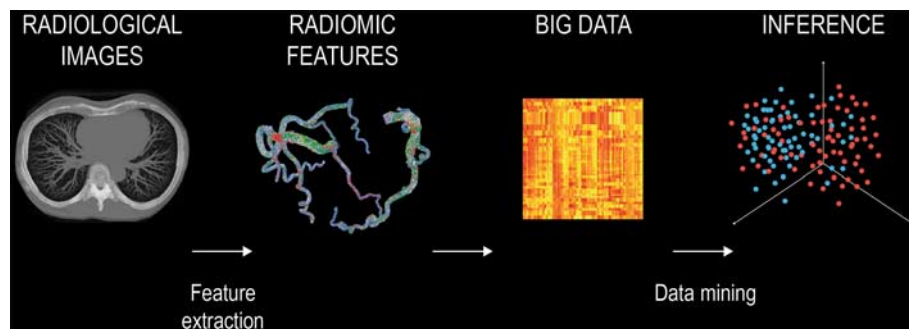


**FIGURE 1.** Pipeline of radiomics-based patient analysis. After image acquisition, new novel radiomics-based image characteristics are extracted to quantify different lesion properties. The hundreds of variables are joined together to create “big data” databases. Data-mining is used to find new meaningful connections between the parameters and the clinical outcome data. On the basis of the results, new imaging biomarkers can be identified that have the potential to increase the diagnostic accuracy of radiologic examinations. full color online

numerous qualitative imaging markers have been identified in coronary CT angiography (CTA).<sup>4,5</sup> These characteristics have been shown to be predictive indicators of subsequent major adverse cardiac events (MACE),<sup>6,7</sup> but they are prone to interobserver and intraobserver variations due to their qualitative nature. It would be highly desirable to use quantitative image parameters instead of qualitative markers to express different lesion characteristics. Radiomics offers mathematical objectivity in describing different lesion characteristics such as heterogeneity, shape, etc.

**CLASSIFICATION OF RADIOMIC TECHNIQUES**

Radiomic techniques can be grouped into 4 major categories: (1) intensity-based metrics, (2) texture-based analysis, (3) shape-based measures, and (4) transform-based metrics. A summary of radiomic techniques can be found in Table 1.

**RADIOMIC TECHNIQUES**

**Intensity-based Metrics**

Intensity-based metrics are often referred to as first-order statistics, which means that statistics are calculated from the voxel values themselves, not considering any additional information that might be gained from analyzing the relationship between the voxels. These statistics can be calculated by selecting a region of interest and extracting the voxel values from it. The values can then be analyzed with the tools of histogram analysis. These statistics can be

grouped into three major categories that quantify different aspects of the distribution: (1) average and variation, (2) shape, and (3) diversity.

**Metrics Representing the Average and Variation of the Data**

Most of these statistics are well known to medical professionals and in some cases are used for describing the characteristics of a coronary lesion: Mean—the most important measure of central tendency that characterizes the voxel values the best as its distance from all other values is minimal. Median—the value that divides the sample into two equal halves. Minimum and maximum—two extreme values of the sample. Percentiles—divide the sample into a given percentage of the data. Interquartile range—two specific values that enclose the middle 50% of the data points. These statistics describe the central tendency of the voxel sample and provide an initial measure of data variation, but they do not provide precise information about the size and shape of the distribution. Several different distributions may exist with the same central tendency but different shapes. Therefore, these statistics are not enough to describe the properties of coronary lesions, as distinct plaque morphologies can have very similar values (Fig. 2).

**Metrics Describing the Shape of the Distribution**

The shape of a distribution is commonly described by moments. Moments are a family of mathematical formulas that capture different properties of the distribution. They are defined as the average of: the voxel values ( $x_i$ ) minus a derived statistic ( $c$ ) raised to a given power ( $q$ ). If  $c = \text{mean } (\mu)$  and  $q = 2$ , then we obtain variance, which provides a measure of sample variation around the mean. The square root of the variance is the standard deviation (SD). In cases of normally distributed data the SD informs us where approximately 68% of the data are located around the mean. If  $c = \mu$ ,  $q = 3$ , and the moment is divided by  $SD^3$ , we obtain skewness, which quantifies how asymmetric the distribution is around the mean. Negative skewness indicates that a large portion of the data are to the right of the mean, whereas positive skewness means the opposite. If  $c = \mu$ ,  $q = 4$ , and the moment is normalized by  $SD^4$ , we obtain kurtosis, which enumerates how close our data points are to the mean. Small values indicate that there are few outliers present in the data and that most values are within one SD of the mean, whereas higher values indicate that a larger number of data points can be found away from

**TABLE 1.** Classification of Different Radiomic Techniques

Intensity-based metrics
Average and spread
Shape
Diversity
Texture-based metrics
Second-order statistics
Higher-order statistics
Laws' texture energy
Shape-based metrics
1D, 2D, 3D
Minkowski functionals
Fractal dimension
Transform-based metrics
Fourier transform
Gabor transform
Wavelet transform

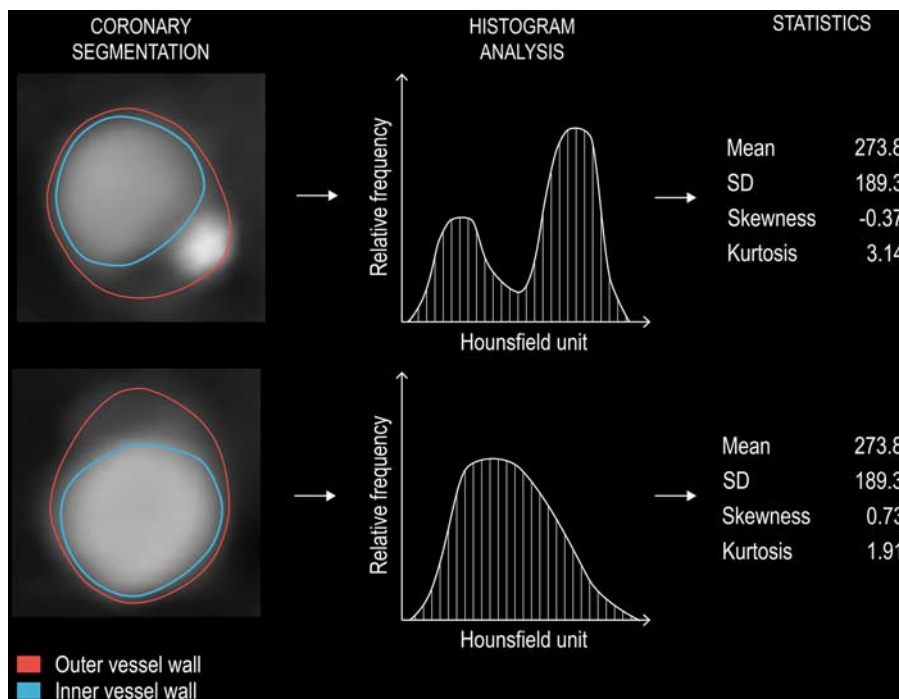


**FIGURE 2.** Pipeline for calculating first-order statistics on two representative examples of coronary lesions. First the coronary arteries need to be segmented. Then histograms need to be created showing the relative frequency of given HU values. From these, different statistics can be calculated. The image also justifies the use of several different parameters to reflect a lesion, as the average attenuation values and the standard deviations are the same, whereas only higher moments can differentiate between these 2 plaques. full color online

the mean beyond one SD. In case of normally distributed data, kurtosis is 3. Thus, it is reasonable to compare the calculated kurtosis with this value to analyze how the data points are distributed around the mean as compared with the normal distribution.

**Metrics Defining the Diversity of Values**

The aforementioned statistics provided information about the average, the variation, and the distribution of the sample but not about the dissimilarity of the voxel values. Concepts from information theory can be used to quantify the heterogeneity of sample values. Energy quantifies the overall magnitude of the intensities and is calculated by squaring the values and then summing them. Uniformity measures the similarity of the values and is calculated by squaring the relative frequency of the given attenuation values and then summing them. Entropy, a concept proposed by Shannon in 1948, measures the information content of our data set.<sup>8</sup> Events with higher probabilities (*p*) carry less information because we can more easily guess their outcome. Conversely, unlikely events carry more information as their occurrence highlights specific instances. Entropy quantifies uncertainty by weighing the information content of an event with its probability. The entropy, hence information content, of a system is equal to the sum of these values multiplied by  $-1$ . The higher the entropy, the more heterogenous the data set. The amount of entropy is commonly measured in bits.

**Applications and Potential Drawbacks**

Even though the concept of radiomics is new, there have been several prior studies exploring the use of quantitative metrics for describing coronary disease. One of the

first quantitative metrics was the Agatston score.<sup>9</sup> The calcium score of a coronary lesion is calculated by taking the area of the lesion and multiplying it by a weighting factor depending on the maximum intensity of the calcified plaque. This simple metric has been demonstrated to be a very good indicator of future MACE and has additive value beyond the traditional risk factors for calculating cardiovascular risk.<sup>10,11</sup>

Unfortunately, there is only limited information about the prognostic value of coronary CTA-derived quantitative intensity-based parameters. Nevertheless, it seems that adding quantitative plaque characteristics to the Framingham risk score and qualitative reading results of medical experts increases the diagnostic accuracy of predicting acute coronary syndrome (area under the curve: 0.64 vs. 0.79,  $P < 0.05$ , respectively).<sup>12</sup>

Quantitative intensity-based metrics have many potential drawbacks. Hounsfield units (HU) are often seen as absolute values, but the truth is that there is a significant amount of variation that can be attributed to different effects. Willemink et al<sup>13</sup> showed that using scanners of different vendors significantly changes the observed Agatston scores of ex vivo hearts (median values: Philips: 353, Toshiba: 410, GE: 469, Siemens: 332;  $P < 0.05$ ). This variation had a significant effect on patient risk stratification, as 6.5% of intermediate-risk patients were reclassified into either a higher-risk or a lower-risk group. In addition, image reconstruction algorithms also affect the observed HU values both in native CT scans and in coronary CTA scans.<sup>14-16</sup> All of these effects limit the use of CTA for identifying different tissue components, which would be crucial for identifying vulnerable plaques. Marwan et al<sup>17</sup> showed that different plaque components

identified by intravascular ultrasound have overlapping HU values on CTA. Thus, the detection of different tissue compartments of plaques is troublesome. This observation led to the use of different cutoff values for different plaque components.<sup>18,19</sup> Furthermore, these results are all based on thousands of voxels sampled on many different individuals. Therefore, if we can see such fluctuations in our values at a population level, then individual variations greatly exceed these, and thus the use of intensity-based metrics for personalized patient-based management becomes highly limited.

All in all, although intensity-based metrics describe the HU distribution of the abnormality, the absence of quantification standards, the uncertainty of reproducibility, and the effects of image reconstruction raise major concerns about the utilization of these metrics for patient management.

### Texture-based Metrics

The above-mentioned parameters discarded all spatial information and used only the absolute values of the voxels themselves, even though we know that the spatial relation of different plaque components has a major effect on plaque vulnerability.<sup>20</sup> Plaque composition is expressed by the spatial relationship of the voxels on CTA. This relationship is hard to conceptualize using mathematical formulas. A solution emerged in the 1970s, when scientists were presented with the problem of identifying different terrain types from satellite images. The field of texture analysis was born and has been evolving ever since. Texture is the broad concept of describing patterns on images. Patterns correspond to the systematic, spatial repetition of some physical

characteristics such as intensity, shape, or color. Texture analysis attempts to quantify these concepts by the use of mathematical formulas based on the spatial relationship of the voxels.

### Second-order Statistics

In 1973, Haralick et al<sup>21</sup> proposed the idea of gray-tone spatial dependencies matrix, commonly known as gray-level co-occurrence matrix (GLCM), for the texture analysis of 2D images. GLCMs are second-order statistics, which means that statistics are calculated from the spatial relationship of two pixel values and not from the values themselves. The goal of these matrices is to quantify how frequently similar value voxels are located next to each other within a given direction and distance and to derive statistics from this information.

In cardiac radiomics, first the coronary arteries need to be segmented to determine the inner and the outer vessel wall boundaries and thereby locate the coronary lesions. Then the HU values of the voxels need to be discretized into a given number of groups, as voxels with exactly the same values occur only very rarely in an image. Our GLCM will have exactly the same number of columns as rows, which equals the number of HU groups we discretized our image to. Next, a direction and a distance need to be determined to examine texture. Direction is usually described with an angle. By convention, voxels to the east of a reference voxel are at 0 degrees, the ones to the north-east are at 45 degrees, the ones to the north are at 90 degrees, and the ones to the north-west are at 135 degrees. One only needs to calculate the statistics in these four directions, as the remaining four

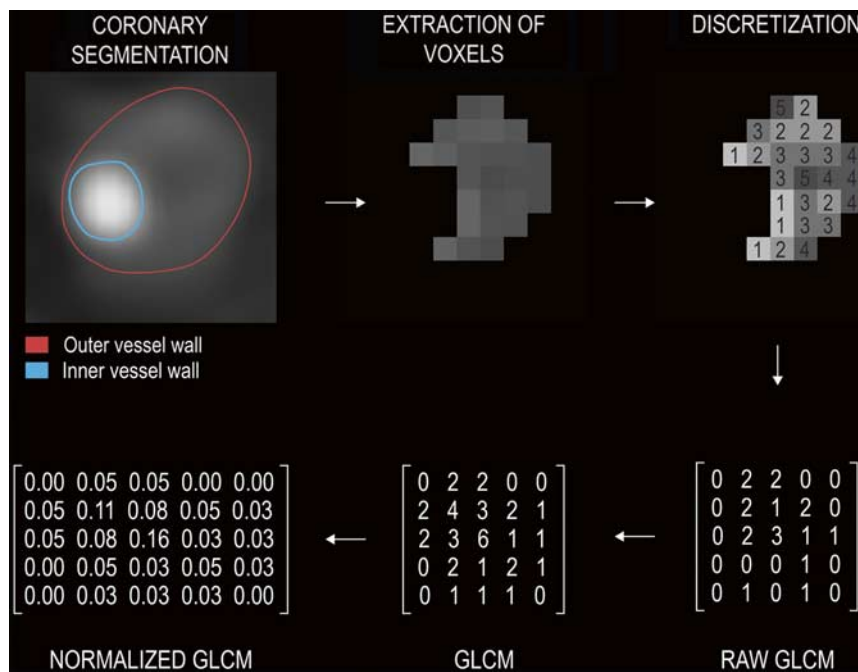


**FIGURE 3.** Pipeline for calculating GLCM. First the coronary arteries need to be segmented. Then the voxels need to be extracted from the images. Next the images need to be discretized into *n* different value groups. Then a given direction and distance is determined to calculate the GLCM (distance 1, angle 0 degrees). Raw GLCMs are created by calculating the number of times a value *j* occurs to the right of value *i*. This value is then inserted into the *i*th row and *j*th column of the raw GLCM. To achieve symmetry, the transpose is added to the raw GLCM. Next, the matrix is normalized by substituting each value by its frequency. This results in the normalized GLCM. Afterward, different statistics can be calculated from the GLCMs. To get rotationally invariant results, statistics are calculated in all four directions and then averaged.

directions are exact counterparts of the above. For example, if our angle equals 0 degrees, and the distance equals 1, then the raw GLCM is created by calculating the number of times a value  $j$  occurs to the right of value  $i$ . This number is then put into the  $i$ th row and  $j$ th column of the raw GLCM. If we were to calculate the GLCM in the opposite direction (at 180 degrees), we would get very similar results so that the rows and columns are interchanged as compared with the original GLCM (at 0 degrees), as asking how many times we find a voxel value  $j$  to the right of voxel value  $i$  is the same as asking how many times we will find a voxel value  $i$  to the left of voxel value  $j$ . Thus, for convenience, we add the transposed matrix (rows and columns are interchanged) to our original raw GLCM matrix to receive a symmetrical GLCM matrix (a value in the  $i$ th row and  $j$ th column equals the value in the  $j$ th row and  $i$ th column). As the absolute numbers are not too informative, we normalize the matrix by dividing all the values in the matrix by the sum of all values in the GLCM to receive relative frequencies instead of absolute numbers. The pipeline for calculating GLCMs can be found in Figure 3.

These matrices contain a lot of information on their own. The values on the main diagonal represent the probabilities of finding identical-value voxels. The further away we move from the main diagonal, the greater the difference between the intensity values. One extreme would be to have only elements on the main diagonal, which would mean that only similar-value voxels are present in that given direction and distance. Another extreme would be if all elements of the GLCM have the same value. In this case the intensity values occur randomly in the image.

Haralick et al proposed 14 different statistics that can be determined from the GLCMs, but many more exist. All derived metrics weigh the entries of the matrix by some value depending on what property one wants to emphasize. Angular second moment/uniformity/energy squares the elements of the GLCM and then sums them up. The fewer the different values present in the matrix, the higher the value of uniformity. Contrast is calculated by multiplying each value of the GLCM by the difference in the attenuation values squared for that given row and column  $(i - j)^2$  and then adding up all the numbers. We receive greater weights when there is a large difference between the

intensity values of the neighboring voxels. A weight of 0 is obtained for elements on the main diagonal when the two voxel intensities are equal. Therefore, contrast quantifies the degree of different HU value voxels present in a given direction and distance. Homogeneity/inverse difference moment uses the reciprocal value of the previous weights. This way, elements closer to the main diagonal receive higher weights, whereas values farther away receive smaller values.

As texture is an intrinsic property of the image, we should not obtain different results even if the image is rotated by 90 degrees. Therefore, to achieve rotationally invariant results, statistics are calculated on the four GLCMs and then averaged.

**Higher-order Statistics**

Whereas second-order statistics examine the relationship between two voxels, higher-order statistics assess the relationship between three or more voxels. The easiest concept proposed by Galloway<sup>21</sup> is the gray-level run-length matrix (GLRLM) that assesses how many voxels are next to each other with the same value. The rows of the matrix represent the attenuation values and the columns the run lengths. The pipeline for calculating GLRLMs can be found in Figure 4.

Galloway proposed 5 different statistics to emphasize different properties of these matrices. Short runs emphasis divides all values by their squared run length and adds them up. The number of short run lengths will hence be divided by a small value, whereas the number of long run lengths will be divided by a large value. Accordingly, the short run lengths will be emphasized. Long runs emphasis carries out just the opposite: instead of dividing the values it multiplies the entries with the squared run length and then adds them up. Gray-level nonuniformity squares the number of run lengths for each discretized HU group and then sums them up. If the run lengths are equally probable in all cases of intensities, it takes up its minimum. Run length non-uniformity carries out just the opposite: it squares the number of run lengths for each run length and then adds them. This measures how equally distributed the run lengths are for all lengths. All these measures can be normalized by the sum of the elements in the GLRLM. Run

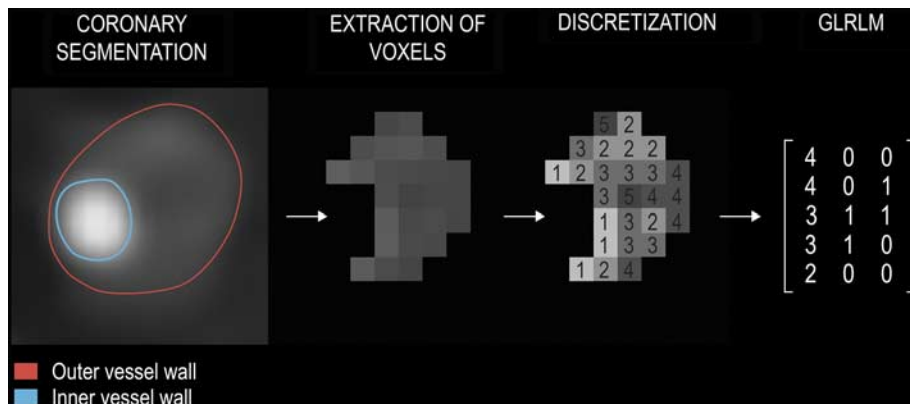


**FIGURE 4.** Pipeline for calculating GLRLM. First, the coronary arteries need to be segmented. Next, the voxels need to be extracted from the images. Then, the images need to be discretized into  $n$  different value groups. Next, a given direction (angle 0 degrees) is determined. GLRLMs are created by calculating the number of times an  $i$  value voxel occurs next to each other in the given direction. The  $i$ th row and  $j$ th column of the GLRLM represents how many times it occurs in the image, that  $i$  value voxels are next to each other  $j$  times. To get rotationally invariant results, the statistics calculated in different directions are averaged.

percentage simply adds the elements of the GLRLM and divides it by the number of voxels. It is smallest in cases when there are only a few long run lengths. These statistics can also be calculated in all 4 directions. To obtain rotationally invariant results, we average them.

GLCMs and GLRLMs have inspired many to create their own matrices on the basis of some other rule. These are, but not limited to, gray-level gap length matrix,<sup>22</sup> gray-level size zone matrix,<sup>23</sup> neighborhood gray-tone difference matrix,<sup>24</sup> or the multiple gray-level size zone matrix.<sup>25</sup>

### Laws' Texture Energy Measures

Laws<sup>26</sup> suggested a different method for quantifying texture. He proposed a method to emphasize different features in the image. The procedure is carried out by convolution, which is the multiplication of the voxel values by values within a neighborhood defined by a weighted kernel, which results in a new image. Depending on the kernel weighting we can filter out certain properties while emphasizing others. Laws proposed 5 different 1D kernels that emphasize some characteristic, such as ripples or edges. These 1D kernels can be used to create 2D and 3D kernels that can alter radiologic images. We can calculate any statistics—for example, energy—on these new images to summarize them.

### Applications and Potential Drawbacks

Texture-based metrics have been used extensively for classifying tumor heterogeneity,<sup>27–29</sup> but these measures have not been implemented in cardiac radiology. This is mainly because coronary lesions are very small as compared with tumors. Most of the aforementioned statistics are only robust in cases of large data sets; thus, the limited spatial resolution of current scanners just might not be sufficient for texture analysis. Furthermore, whereas tumors are rotationally invariant, and hence any anatomic plane can characterize their heterogeneity well, atherosclerotic lesions are not. Therefore, heterogeneity needs to be assessed along the coronary artery or in 3D.

### Shape-based Metrics

Atherosclerotic plaques are complex 3D structures situated along the coronary arteries. The spatial distribution and localization of different plaque components can also have an effect on plaque vulnerability.

#### 1D Metrics

1D metrics are based on measuring the distance between 2 points. These parameters are commonly used in clinical practice to describe the magnitude of an abnormality. On coronary arteries the diameter stenosis is used to assess the severity of a lesion, or the length to quantify the extent of a plaque. Diameters measured in different directions can be used to derive new statistics that can resemble some new property. For example, the ratio of the longest and the shortest diameters describes the roundedness or ellipticity of a lesion.

#### 2D Metrics

2D metrics are calculated on cross-sectional planes and are used to calculate different parameters that are based on areas. These parameters are most often used to approximate some 3D property of the abnormality. For example, the 1D metric diameter and the 2D metric area are all considered approximations of the 3D metric volume.

Accordingly, cross-sectional plaque burden is used to approximate full vessel volume-based plaque burden in coronary CTA.

### 3D Metrics

3D metrics attempt to enumerate different aspects of volumetric shape. The geometrical properties of shapes have been thoroughly examined in the field of rigid-body mechanics. All objects have so-called principal axes or eigenvectors. These mutually perpendicular axes cross each other at the center of mass. The force applied to the axes act independently, meaning that if we push or rotate the object along or around any of these principal axes our object will not move or rotate in any other direction. These eigenvectors also have eigenvalues that can be seen as weights proportional to the amount of mass or in our case the HU intensity located in that given principal axis. The eigenvectors can be used to quantify different shape-based metrics—for example, roundedness, which is the difference between the largest eigenvalues of the smallest enclosing and the largest enclosed ellipse.

### Minkowski Functionals

Minkowski functionals originate from integral geometry.<sup>30</sup> They can be used to calculate different properties of geometrical objects, such as the Euler characteristic or genus, which is a parameter describing the connectivity of the data points. Connectivity is estimated by calculating the number of voxel groups with information minus the enclosed regions where there is no signal.<sup>31</sup> By taking a different threshold of our image we can calculate different parameters for each image. These values can be used to describe the connectivity of different intensity values in the image.

### Fractal Dimension

Fractal geometry quantifies self-symmetry by examining repeating patterns at different scales. Objects with no fractal properties scale their characteristics exponentially depending on the dimension. For example, if we enlarge a line by 2, considering that the line is a 1D object, its length will increase to 2<sup>1</sup>. If we scale one side of a square by 2, then the area of the square will increase by 2<sup>2</sup> as it is a 2D object. A cube's volume would increase to 2<sup>3</sup> if we increased all of its sides by 2. However, fractals act differently. If we were to enlarge a line that has fractal properties by 2, then its length would not be twice as long as it would be for a line without fractal properties, but longer. This is because when we magnify an object with fractal properties we start to see more and more details, which affects the length of the given object. This can be better seen when trying to measure the length of a coastline. When we magnify our image more and more, we begin to see more and more details, which affects the total measured length, and therefore the total length of the coastline increases.

Fractal dimensions measure the self-symmetry of objects and quantify how the detail of the object changes as we change our scale.<sup>32</sup> Rényi dimensions can be used to calculate fractal dimensions generally. The box-counting dimension or Minkowski–Bouligand dimension is the easiest concept. We calculate how many voxels are occupied by the object. We repeat this at increasing scales. Then we plot the number of voxels containing the object versus the reciprocal of the scale on a log–log plot. The slope of the line will be equal to the box-counting dimension.<sup>33,34</sup>

## Applications and Potential Drawbacks

In clinical routine, mainly 1D metrics are used to assess plaque stenosis severity and other characteristics of coronary lesions. Stenosis severity is commonly expressed as diameter stenosis, which is the ratio of the smallest lumen diameter to a reference value. Several studies have investigated the effect of diameter stenosis on subsequent outcome, but long-term effects still remain a question.<sup>35</sup> Lesion length, another 1D metric, has also been investigated and has been shown to correlate with MACE in patients undergoing percutaneous coronary intervention.<sup>36</sup> 2D metrics based on cross-sectional area are used to describe positive remodeling, which is the vessel cross-sectional area at maximal stenosis divided by the mean of the proximal and distal reference sites' cross-sectional areas.<sup>37</sup> The remodeling index has been shown to be an independent vulnerability feature of vulnerable plaques.<sup>38</sup> Among 3D metrics, volume is used to express the magnitude of coronary disease. Versteyleen et al<sup>12</sup> showed that total plaque volume, total noncalcified volume, per-plaque maximal volume, noncalcified percentage, and plaque burden are significantly larger in acute coronary syndrome patients as compared with that in nonacute coronary syndrome controls.

Shape-based metrics have the advantage of being easily comprehensible, and many of them can be calculated in daily clinical routine. The only concern is that coronary lesions grow along coronary arteries; thus, when we are trying to observe the shape of a lesion, we might be measuring some aspect of the coronary geometry. Therefore, it is hard to assess plaque shape independent of coronary geometry. This actually might not be a problem, as the effect of coronary curvature on plaque vulnerability has been extensively investigated through computational fluid dynamics and appears to affect plaque formation and vulnerability.<sup>39</sup>

## Transform-based Metrics

An image is a vast number of pixel/voxel values distributed along spatial coordinates, hence in the spatial domain. The image can be transformed into the so-called frequency domain without losing any information. The spatial-domain and frequency-domain representations of an image carry identical information, but they emphasize different features and offer different computational possibilities. In the frequency domain, the pattern and rate at which the image intensity values change along spatial directions are used to present the image rather than by assigning intensity values to spatial coordinates.

## Fourier and Gabor Transforms

Fourier transform decomposes the spatial-domain data set into a fundamental sine wave and its harmonics along the two dimensions of an image. The 2D Fourier transform (or most commonly the fast Fourier transform) displays the amplitude of the Fourier component, represented in grayscale or color, as a function of frequency. Once converted into the frequency domain, spatial information—that is, the spatial location of specific frequencies—is lost. The Gabor transform, so named after the Hungarian-born physicist Denes Gabor, is a special case of the Fourier transform in which spatial and frequency information can be treated simultaneously; thus space-dependent frequency features can also be extracted. In Gabor transform, the Fourier transform is preceded by

filtration with a Gaussian kernel (or a sinusoidally modulated Gaussian function called Gabor wavelet; see below). Whereas fast Fourier transform allows the identification and hence the filtration of specific frequencies (eg, ones related to noise), Gabor transform provides access to image features such as edges, texture, blobs, and even face recognition. Carrying out the inverse transformations converts the transforms back to the spatial domain.

## Wavelet Transforms

Wavelet transforms are similar to Fourier transforms in that they also convert the image into the frequency domain, but spatial information is retained.<sup>40</sup> Wavelet transforms are rooted in the so-called windowed Fourier transform, in which a window function is translated across the original function, the image in our case. The width of the window determines both the spatial resolution (localization precision) and the frequency resolution (global image features): the narrower the window, the greater the localization precision (poorer the frequency resolution) and vice versa, in a way similar to the Heisenberg uncertainty principle. If the window has a fixed size and contains a Gaussian function, then the Gabor transform is obtained (see above) providing fixed space-frequency resolution. To achieve multiresolution, a scalable and translatable function called the wavelet is applied. The use of wavelets assists in the denoising, compression, and fusion of images.

## Applications and Potential Drawbacks

Fourier and Gabor transforms are widely used in image processing for filtering the images of different spatial frequencies and for extracting certain features. Wavelet transforms are increasingly being used to describe different properties of the spatial and frequency components of medical abnormalities.<sup>41</sup> Numerous statistics can be gained from these transforms by setting different parameter values; therefore, thorough investigation of predictors is needed to account for model overfitting.

## Potential Difficulties of Implementing Radiomics in the Clinical Routine

Radiomics is a captivating new discipline with the potential to increase our knowledge in medicine and the efficacy of our clinical decisions. However, first, standardized acquisition protocols and data analysis techniques need to be established to provide a robust framework for radiomics analysis. Recently the Radiological Society of North America (RSNA) initiated the Quantitative Imaging Biomarkers Alliance (QIBA) to facilitate the development and deployment of radiomics. Similarly, the European Society of Radiology (ESR) introduced the European Imaging Biomarkers Alliance (EIBALL) to improve the standardization and performance of quantitative imaging parameters. Once these standards are well established, radiomics still has to overcome its technical complexity to be useful in daily clinical routine. User-friendly automated software solutions need to be developed that can extract and evaluate these new imaging biomarkers without increasing the burden on the radiologist. Furthermore, we must not forget that radiomics creates huge data sets that need to be analyzed, which is very time-consuming and potentially further increases the workload of radiologists. Therefore, robust software solutions need to be developed capable of implementing radiomics in the daily clinical

routine without increasing the clinical load. Without this, radiomics might remain a toll of the researchers.

## CONCLUSIONS

The demand for radiologic examinations is increasing worldwide. However, not only the number but also the complexity of new imaging modalities greatly increases the burden of radiologists. Furthermore, in the new millennium where everything is about acquiring more and more information, the interpretation of radiologic images needs to be reformed. Although visual inspection might be suitable for clinical diagnosis, there is a growing need for quantitative image analysis techniques that can further increase our understanding of diseases and the precision of our examinations. Radiologic examinations are vast spatial data sets, where every voxel is a measurement itself. The emerging field of radiomics tries to utilize this information by quantifying spatial and textural properties that are difficult to discern by the naked eye. These new imaging biomarkers have the potential to objectify our interpretation of medical images and increase the diagnostic accuracy of our examinations. However, as with all new technologies, we currently lack sufficient scientific results supporting these claims. The expectations of radiomics are high, but if successful the consequences might be even higher.

## REFERENCES

1. Thomas A, Banerjee AK, Gardner-Thorpe C. The history of radiology. 1st ed Oxford: Oxford University Press; 2013. xiii, 222 pp.
2. Jones BK, Buckwalter AJ, McCarthy FE, et al. Reliability of histopathologic and radiologic grading of cartilaginous neoplasms in long bones. *J Bone Joint Surg Am.* 2007;89:2113–2123.
3. Barabasi AL, Gulbahce N, Loscalzo J. Network medicine: a network-based approach to human disease. *Nat Rev Genet.* 2011;12:56–68.
4. Maurovich-Horvat P, Hoffmann U, Vorpahl M, et al. The napkin-ring sign: CT signature of high-risk coronary plaques? *JACC Cardiovasc Imaging.* 2010;3:440–444.
5. Maurovich-Horvat P, Ferencik M, Voros S, et al. Comprehensive plaque assessment by coronary CT angiography. *Nat Rev Cardiol.* 2014;11:390–402.
6. Otsuka K, Fukuda S, Tanaka A, et al. Napkin-ring sign on coronary CT angiography for the prediction of acute coronary syndrome. *JACC Cardiovasc Imaging.* 2013;6:448–457.
7. Shannon CE. A mathematical theory of communication. *The Bell Syst Tech J.* 1948;27:379–423.
8. Agatston AS, Janowitz WR, Hildner FJ, et al. Quantification of coronary artery calcium using ultrafast computed tomography. *J Am Coll Cardiol.* 1990;15:827–832.
9. Polonsky TS, McClelland RL, Jorgensen NW, et al. Coronary artery calcium score and risk classification for coronary heart disease prediction. *JAMA.* 2010;303:1610–1616.
10. McClelland RL, Jorgensen NW, Budoff M, et al. 10-year coronary heart disease risk prediction using coronary artery calcium and traditional risk factors: derivation in the MESA (Multi-Ethnic Study of Atherosclerosis) with validation in the HNR (Heinz Nixdorf Recall) Study and the DHS (Dallas Heart Study). *J Am Coll Cardiol.* 2015;66:1643–1653.
11. Versteijlen MO, Kietselaer BL, Dagnelie PC, et al. Additive value of semiautomated quantification of coronary artery disease using cardiac computed tomographic angiography to predict future acute coronary syndrome. *J Am Coll Cardiol.* 2013;61:2296–2305.
12. Willemink MJ, Vliegenthart R, Takx RA, et al. Coronary artery calcification scoring with state-of-the-art CT scanners from different vendors has substantial effect on risk classification. *Radiology.* 2014;273:695–702.
13. Szilveszter B, Elzomor H, Karolyi M, et al. The effect of iterative model reconstruction on coronary artery calcium quantification. *Int J Cardiovasc Imaging.* 2016;32:153–160.
14. Precht H, Kitslaar PH, Broersen A, et al. Influence of Adaptive Statistical Iterative Reconstruction on coronary plaque analysis in coronary computed tomography angiography. *J Cardiovasc Comput Tomogr.* 2016;10:507–516.
15. Fuchs TA, Fiechter M, Gebhard C, et al. CT coronary angiography: impact of adapted statistical iterative reconstruction (ASIR) on coronary stenosis and plaque composition analysis. *Int J Cardiovasc Imaging.* 2013;29:719–724.
16. Marwan M, Taher MA, El Meniawy K, et al. In vivo CT detection of lipid-rich coronary artery atherosclerotic plaques using quantitative histogram analysis: a head to head comparison with IVUS. *Atherosclerosis.* 2011;215:110–115.
17. Takahashi S, Kawasaki M, Miyata S, et al. Feasibility of tissue characterization of coronary plaques using 320-detector row computed tomography: comparison with integrated backscatter intravascular ultrasound. *Heart Vessels.* 2016;31:29–37.
18. Brodoefel H, Reimann A, Heuschmid M, et al. Characterization of coronary atherosclerosis by dual-source computed tomography and HU-based color mapping: a pilot study. *Eur Radiol.* 2008;18:2466–2474.
19. Virmani R, Burke AP, Farb A, et al. Pathology of the vulnerable plaque. *J Am Coll Cardiol.* 2006;47(Suppl):C13–C18.
20. Haralick RM, Shanmugam K, Dinstein I. Textural Features for Image Classification. *IEEE Transactions on Systems, Man, and Cybernetics.* 1973;SMC-3(6):610–621.
21. Galloway MM. Texture analysis using gray level run lengths. *Comput Graphics Image Process.* 1975;4:172–179.
22. Xinli W, Albrechtsen F, Foyn B. *Texture Analysis Using Gray Level Gap Length Matrix Selected Papers From the 9th Scandinavian Conference on Image Analysis: Theory and Applications of Image Analysis II: Theory and Applications of Image Analysis II.* Uppsala, Sweden: World Scientific Publishing Co., Inc.; 1995:65–78.
23. Thibault G, Fertil B, Navarro C, et al. Shape and texture indexes application to cell nuclei classification. *IJPRAI.* 2013;27:1357002.
24. Amadasun M, King R. Textural features corresponding to textural properties. *IEEE Trans Syst Man Cybern.* 1989;19:1264–1274.
25. Thibault G, Angulo J, Meyer F. Advanced statistical matrices for texture characterization: application to cell classification. *IEEE Trans Biomed Eng.* 2014;61:630–637.
26. Laws KI. Textured Image Segmentation. *University of Southern California, 1980. Textured Image Segmentation.* University of Southern California: Pages: viii, 1–178.
27. O'Connor JP, Rose CJ, Waterton JC, et al. Imaging intratumor heterogeneity: role in therapy response, resistance, and clinical outcome. *Clin Cancer Res.* 2015;21:249–257.
28. Davnall F, Yip CS, Ljungqvist G, et al. Assessment of tumor heterogeneity: an emerging imaging tool for clinical practice? *Insights Imaging.* 2012;3:573–589.
29. Parmar C, Rios Velazquez E, Leijenaar R, et al. Robust Radiomics feature quantification using semiautomatic volumetric segmentation. *PLoS One.* 2014;9:e102107.
30. Minkowski H. Volumen und Oberfläche. *Math Ann.* 1903;57:447–495.
31. Larkin TJ, Canuto HC, Kettunen MI, et al. Analysis of image heterogeneity using 2D Minkowski functionals detects tumor responses to treatment. *Magn Reson Med.* 2014;71:402–410.
32. Mandelbrot B. How long is the coast of Britain? Statistical self-similarity and fractional dimension. *Science.* 1967;156:636–638.
33. Rose CJ, Mills SJ, O'Connor JP, et al. Quantifying spatial heterogeneity in dynamic contrast-enhanced MRI parameter maps. *Magn Reson Med.* 2009;62:488–499.

34. Lopes R, Betrouni N. Fractal and multifractal analysis: a review. *Med Image Anal.* 2009;13:634–649.
35. Kolossvary M, Szilveszter B, Merkely B, et al. Plaque imaging with CT—A comprehensive review on coronary CT angiography based risk assessment. *Cardiovasc Diagn Ther.* 2017. DOI: 10.21037/cdt.2016.11.06.
36. Claessen BE, Smits PC, Kereiakes DJ, et al. Impact of lesion length and vessel size on clinical outcomes after percutaneous coronary intervention with everolimus- versus paclitaxel-eluting stents pooled analysis from the SPIRIT (Clinical Evaluation of the XIENCE V Everolimus Eluting Coronary Stent System) and COMPARE (Second-generation everolimus-eluting and paclitaxel-eluting stents in real-life practice) Randomized Trials. *JACC Cardiovasc Interv.* 2011;4:1209–1215.
37. Achenbach S, Ropers D, Hoffmann U, et al. Assessment of coronary remodeling in stenotic and nonstenotic coronary atherosclerotic lesions by multidetector spiral computed tomography. *J Am Coll Cardiol.* 2004;43:842–847.
38. Motoyama S, Kondo T, Sarai M, et al. Multislice computed tomographic characteristics of coronary lesions in acute coronary syndromes. *J Am Coll Cardiol.* 2007;50:319–326.
39. Slager CJ, Wentzel JJ, Gijsen FJ, et al. The role of shear stress in the generation of rupture-prone vulnerable plaques. *Nat Clin Pract Cardiovasc Med.* 2005;2:401–407.
40. Dettori L, Semler L. A comparison of wavelet, ridgelet, and curvelet-based texture classification algorithms in computed tomography. *Comput Biol Med.* 2007;37:486–498.
41. Balagurunathan Y, Kumar V, Gu Y, et al. Test-retest reproducibility analysis of lung CT image features. *J Digit Imaging.* 2014;27:805–823.